

CHAPTER 3

Application of Recurrence Quantification Analysis: Influence of Cognitive Activity on Postural Fluctuations

Geraldine L. Pellecchia

Department of Physical Therapy
School of Allied Health
University of Connecticut
358 Mansfield Rd., Unit 2101
Storrs, CT 06269-2101
U. S. A.
E-mail: geraldine.pellecchia@uconn.edu

Kevin Shockley

Department of Psychology
University of Cincinnati
ML 0376, 429 Dyer Hall
Cincinnati, OH 45221-0376
U. S. A.
E-mail: kevin.shockley@.edu

Control of a stable standing posture is requisite to many everyday actions. During upright standing, the body undergoes continuous, low-amplitude sway. These spontaneous postural fluctuations are often indexed by the center of pressure (COP). The COP is the location of the net vertical ground reaction force and is calculable from the forces and moments measured by a device called a force platform. During upright standing with equal weight bearing on each foot, the COP is located midway between the feet. The path traversed by the COP over time reflects the dynamic nature of postural control. Figure 3.1 depicts a typical COP path during 30 s of upright standing on a compliant surface. The ease with which COP measures can be obtained with a force platform provides a means to explore factors that may influence postural control.

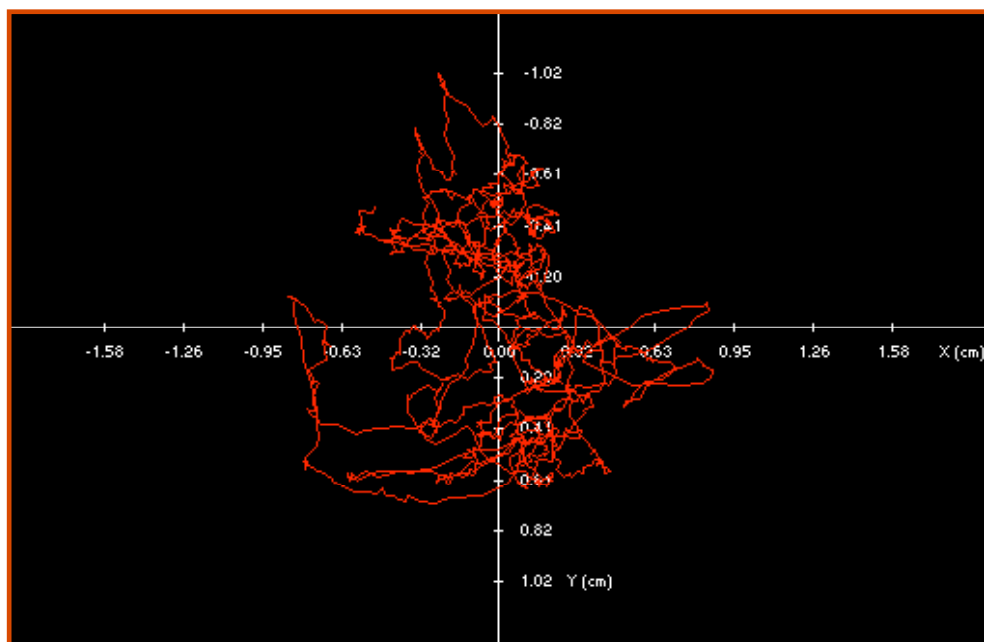


Figure 3.1. A sample 30 s center of pressure (COP) profile. COP path is shown for an individual standing upright with feet together on a compliant surface.

An important aspect of many routine activities of daily living is the ability to concurrently maintain an upright posture and perform an unrelated cognitive task. For example, we often walk while talking. Despite that such scenarios are commonplace, executing cognitive and postural tasks concurrently is not without consequence. Numerous studies have demonstrated changes in performance on either the cognitive, postural, or both tasks when carried out simultaneously compared to when the same tasks are performed separately (e.g., Dault, Geurts, Mulder, & Duysens, 2001; Kerr, Condon, & McDonald, 1985; Lajoie, Teasdale, Bard, & Fleury, 1993; Maylor, Allison, & Wing, 2001; Maylor & Wing, 1996; Stelmach, Zelaznik, & Lowe, 1990).

In a recent paper, Pellecchia (2003) examined the effect of attentional demand on postural sway. COP was recorded as participants stood on a force platform and performed cognitive tasks that varied in attentional requirements. Attentional demand was quantified using information reduction tasks modeled after those described by Posner (1964; Posner & Rossman, 1965). An information reduction task is one in which the required cognitive operation results in a reduction of information from stimulus to response. The size of that transformation is quantified by the difference in the amount of information contained in the stimulus and the response. Posner asserted that the attentional requirements of a cognitive task could be manipulated by varying the processing demands of the task. For a set of numeric tasks, Posner demonstrated a direct relation between task difficulty and the magnitude of information reduced in carrying out a task. Information reduction tasks have been an effective means of

manipulating the attentional requirements of cognitive activity (for an example, see Pellecchia & Turvey, 2001).

To examine the influence of attentional demand on postural sway, Pellecchia (2003) adopted a conventional approach to data analysis. Specifically, the mean magnitude and variability of the COP path during upright standing were compared across a set of information reduction tasks. This traditional method has been used extensively in previous studies examining effects of various experimental manipulations on postural control (for examples, see Derave, De Clercq, Bouckaert, & Pannier, 1998; Gravelle et al., 2002; Guerraz, Thilo, Bronstein, & Gresty, 2001; Polonyova & Hlavacka, 2001; Vuillerme, Forestier, & Nougier, 2002; Vuillerme, Nougier, & Teasdale, 2000). Although well established, this approach to the analysis of COP data is of limited usefulness. Summary measures of COP path magnitude and variability do not reflect the dynamical properties of postural control (Newell, 1998). In contrast, recurrence quantification analysis (RQA), a relatively new analytical method, examines the time evolution of data series (see Webber & Zbilut, Chapter 2). In recent years, investigators have begun using RQA to explore the dynamics of postural control. For example, Riley and Clark (2003) employed RQA to investigate how changes in sensory information influenced the temporal structure of spontaneous postural sway, and thereby to gain insight into the adaptive nature of postural control. RQA is a useful tool for identifying structure that is inherent in postural fluctuations but not evident when using conventional methods of analyzing COP data. The purpose of this chapter is to demonstrate the application of RQA to the study of postural fluctuations during standing as a function of varying

attentional demands of an unrelated, concurrent, cognitive task. Following a description of the experimental method, we review the results of the traditional analysis of COP data as previously reported by Pellecchia (2003). Next, we employ the methods of RQA to examine the dynamical properties of COP time series.

COGNITIVE ACTIVITY & POSTURAL CONTROL: THE EXPERIMENT

An AMTI Accusway System for Balance and Postural Sway Measurement (Advanced Mechanical Technology, Inc., Watertown, Massachusetts) was used to collect data. The Accusway System consists of a portable force platform and *SWAYWIN* software for data acquisition and analysis. The force platform produces six signals—three force measures, F_x , F_y , and F_z , and three moment measures, M_x , M_y , and M_z , where the subscripts x, y, and z denote medio-lateral (ML; side-to-side), anterior-posterior (AP; front-to-back), and vertical directions, respectively. *SWAYWIN* software uses the forces and moments to calculate x and y coordinates of the position of the COP. The Accusway System samples at a rate of 50 Hz. Therefore, a 30 s trial period yielded 1500 data points for the ML COP (position of the center of pressure in the ML direction) time series and 1500 data points for the AP COP (position of the center of pressure in the AP direction) time series.

The postural task consisted of standing on a 10 cm thick foam pad that had been placed on top of the force platform, as shown in Figure 3.2. The foam pad created a compliant surface, thereby altering the somatosensory information available for postural control and making the postural task more challenging than simply standing on a firm, flat surface.



Figure 3.2. The experimental set-up used in the present experiment. Participants stood with feet together, arms by side, and looking straight ahead at a blank wall. A foam pad was placed on the force platform to create a compliant surface.

Three information reduction tasks—digit reversal, digit classification, and counting backward by 3s—were used to vary the attentional demands of the concurrent cognitive task. The amount of information reduced in performing each task was determined using the method described by Posner (1964; Posner & Rossman, 1965; see also Note 1 in Pellecchia & Turvey, 2001). In digit reversal, the task was to reverse the order of a pair of digits. For example, on hearing the

stimulus 4, 7, a correct response would be 7, 4. The input contained 6.5 bits of information, and the output contained 6.5 bits of information. Therefore, digit reversal was a 0-bit reduction task. In digit classification, the task was to combine a pair of single digits into a double-digit number and to classify that number as high (if > 50) or low (if < 50), and odd or even. For example, the single digits 4, 7, combine to form the double-digit number 47; correct classification would be *low, odd*. The input contained 6.5 bits of information; the output contained 2 bits of information. Therefore, digit classification required 4.5 bits of information reduction. In the counting back by 3s task, participants were given a 3 digit number from which to start counting. Participants were instructed to first recite the starting number, and then count backward by 3s from that number. Correct responses to the stimulus 365 would be 365, 362, 359, 356, and so on. We determined that counting back by 3s from a randomly chosen three-digit number required approximately 5.9 bits of information reduction.

A pre-recorded audiotape provided stimuli for the digit reversal and digit classification tasks. The audiotape consisted of pairs of random single digits presented at a rate of 2 digits/s with a 2 s pause between pairs. For the counting backward by 3s task, a different starting number was selected for each trial. Starting numbers ranging between 200 and 999 were chosen from a random number table. Prior to data collection, participants practiced the three information reduction tasks for a minimum of 15 s each while seated in a chair.

During the experiment, participants stood in stocking feet on the foam pad that rested on the force platform. The force platform was positioned approximately 2 m from a blank wall. Participants were

instructed to stand with the feet together, the arms by the sides, and with the eyes open and looking straight ahead. COP data were collected under four cognitive task conditions: Quiet standing (i.e., performing no cognitive task), standing combined with digit reversal, standing combined with digit classification, and standing combined with counting backward by 3s. Participants performed two 30 s trials of each condition, for a total of eight trials. The order of the four experimental conditions was randomized. Data collection for each participant's first trial began 30-60 s after the participant assumed the proper position on the force platform. For those trials in which standing was combined with a cognitive task, force platform data collection began after the participant voiced their first response. There was a 30-60 s break between trials, during which time the participant remained standing on the platform. Participants' verbal responses to the cognitive tasks were audiotape-recorded for subsequent analysis. Practice and data collection together lasted approximately 30 min.

TRADITIONAL APPROACH TO ANALYSIS OF COP DATA

Data Analysis

SWAYWIN software was used to calculate five dependent measures: Total COP path length (LCOP), antero-posterior (AP) and medio-lateral (ML) COP range, and AP and ML COP variability. LCOP is the total distance traveled by the COP over the 30 s trial period (see Figure 3.1 for a visual display of LCOP). AP COP range and ML COP range are the differences between the two extreme position values in the respective directions. AP and ML COP variability are the standard deviations of the COP in the respective directions. Means of those

quantities were calculated for the two trials in each experimental condition, and the means were used in all subsequent analyses. Separate repeated-measures analyses of variance (ANOVA) were used to determine the effect of cognitive task condition on each COP measure. Pearson product-moment correlations examined the relation between bits of information reduced and each dependent variable.

To examine performance on the cognitive tasks, the number of errors was determined for each trial by listening to the audiotape recording of participants' responses. Error rate was calculated as the number of errors divided by the total number of responses for each 30 s trial. Error rates were averaged for each participant's two trials in each experimental condition. The mean error scores were used in subsequent repeated measures ANOVAs to examine cognitive task performance. Post-hoc analyses were conducted using least significant difference pair-wise multiple comparison tests.

Results of Traditional Analyses

The effects of attentional requirements on postural sway and cognitive task performance were previously reported (Pellecchia, 2003) and are summarized in Figure 3.3. Repeated-measures ANOVAs revealed a main effect of cognitive task condition on LCOP, $F(3, 57) = 8.09, p < .001$, as shown in Figure 3.3a. Figures 3.3b-e depict similar results for the other four COP measures. Separate ANOVAs revealed a main effect of cognitive task condition on AP range $F(3, 57) = 9.84, p < .001$, ML range $F(3, 57) = 3.03, p < .05$, and AP variability, $F(3, 57) = 5.70, p < .01$. Post-hoc tests showed sway measures of LCOP, AP range, ML range, and AP variability were greater for the counting back by 3s

RQA of Postural Fluctuations

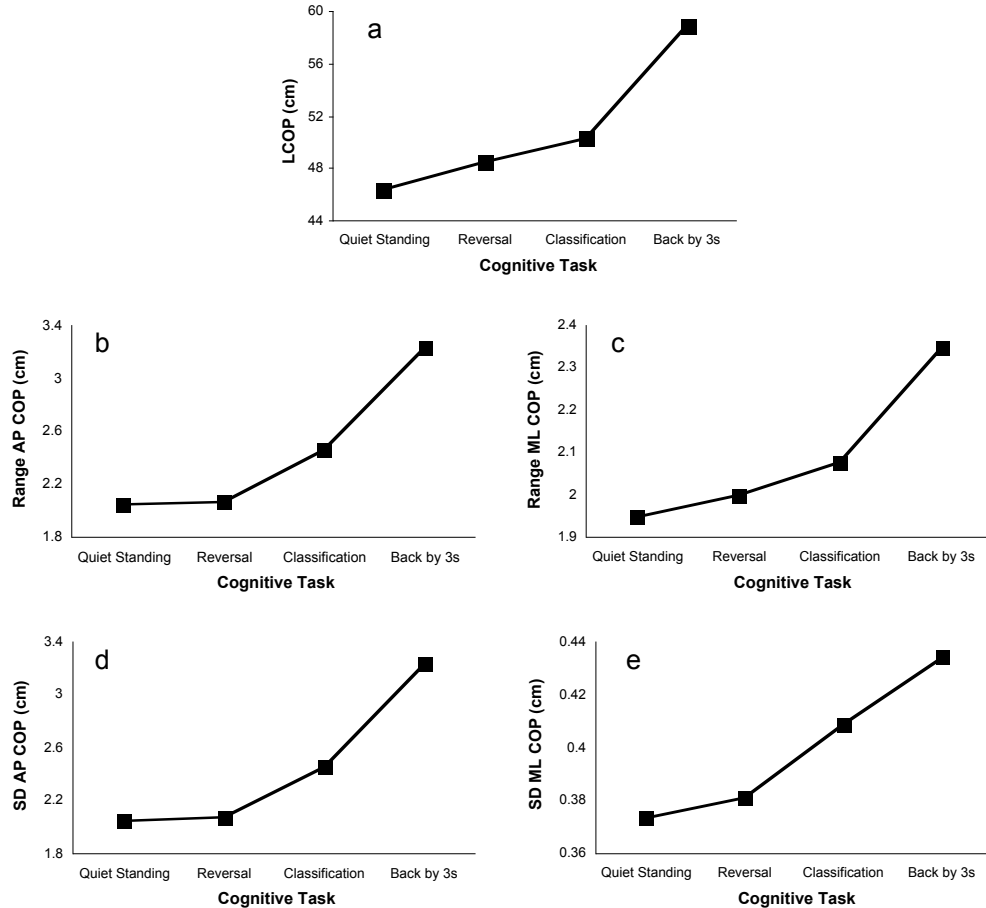


Figure 3.3. Five summary measures of the center of pressure (COP) as a function of cognitive task condition. (a) Total length of the path of the center of pressure (LCOP); (b) Range of COP motion in the anterior-posterior (AP) direction; (c) Range of COP motion in the medio-lateral (ML) direction; (d) standard deviation (SD) of AP COP motion; and (e) SD of ML COP motion.

task than for the other three cognitive task conditions. In addition, AP sway range was greater for digit classification than for quiet standing. For ML variability, the main effect of cognitive task condition approached statistical significance, $F(3, 57) = 2.35, p = .08$. Pair-wise

comparisons suggested greater ML variability for the counting back by 3s task than for digit reversal ($p < .05$) and quiet standing ($p = .06$).

As noted previously, digit reversal, digit classification, and counting back by 3s required 0, 4.5, and 5.9 bits of information reduction, respectively. Inspection of Figures 3.3a-e suggests that postural sway was directly related to the magnitude of information reduced for the cognitive tasks. Separate correlation analyses confirmed this relation between bits of information reduced and each COP measure. Specifically, Pearson correlation coefficients for LCOP, AP range, ML range, AP variability, and ML variability were .79, .89, .82, .89, and .97, respectively.

In the evaluation of cognitive task performance, repeated measures ANOVA revealed a main effect of cognitive task on error rate, $F(2, 36) = 7.58, p < .01$. The error rate for counting back by 3s ($M = 0.113$) was greater than error rates for digit classification ($M = 0.026$) and digit reversal ($M = 0.003$).

To summarize, the traditional approach to analysis of COP data revealed greater magnitude and variability of COP motion with higher attentional demands of a concurrent, unrelated, cognitive task. Upon further inspection of Figures 3.3a-e, the various COP measures appear to provide redundant information. In fact, these measures are highly correlated. Pearson correlation coefficients examining the relation among mean values of the five COP measures ranged from .96 to .99.

Discussion of Results of Traditional Analysis

Considering the results of the traditional analysis of COP data, one might assume that only a single measure of the COP need be considered. That is, each summary measure of the COP suggested a

similar conclusion about the influence of attentional requirements on postural sway. More specifically, performing a concurrent cognitive task was associated with increases in all five measures. Furthermore, there were no apparent differential effects of attentional demands on AP or ML COP motion.

A conventional viewpoint holds that the degree of postural sway reflects performance of the postural control system. In individuals free of neuromuscular or balance disorders, small amplitude and variability of COP excursions is considered to indicate *good* balance, whereas large amplitude and variability of COP motion is considered to indicate *poor* balance. From this perspective, the observed increases in sway magnitude and variability in the present experiment suggest that carrying out a concurrent cognitive task compromises postural stability. Consistent with this view and the traditional notion of attention as limited capacity or limited processing resources, one might conclude that counting backward by 3s while standing upright exceeds an individual's attentional capacity, and brings about a decline in performance of the postural control system (Woollacott & Shumway-Cook, 2002). This interpretation is intuitively appealing and broadly held. On second blush, however, the notion that concurrent performance of a fundamental motor task such as maintaining an upright posture and a relatively simple arithmetic task could exceed human attentional resources is somewhat suspect.

The traditional approach to the analysis of COP data provides limited information about the postural control system's response to concurrent performance of an unrelated cognitive task. In particular, summary measures of COP magnitude and variability do not inform

about the temporal structure of the COP time series. Consider Figure 3.4, which depicts the AP COP and ML COP time series for the COP profile shown in Figure 3.1. Using the methods of RQA, we can explore the temporal structure of these postural fluctuations, and perhaps gain further insight into changes brought about in the postural control system by varying the attentional requirements of cognitive activity.

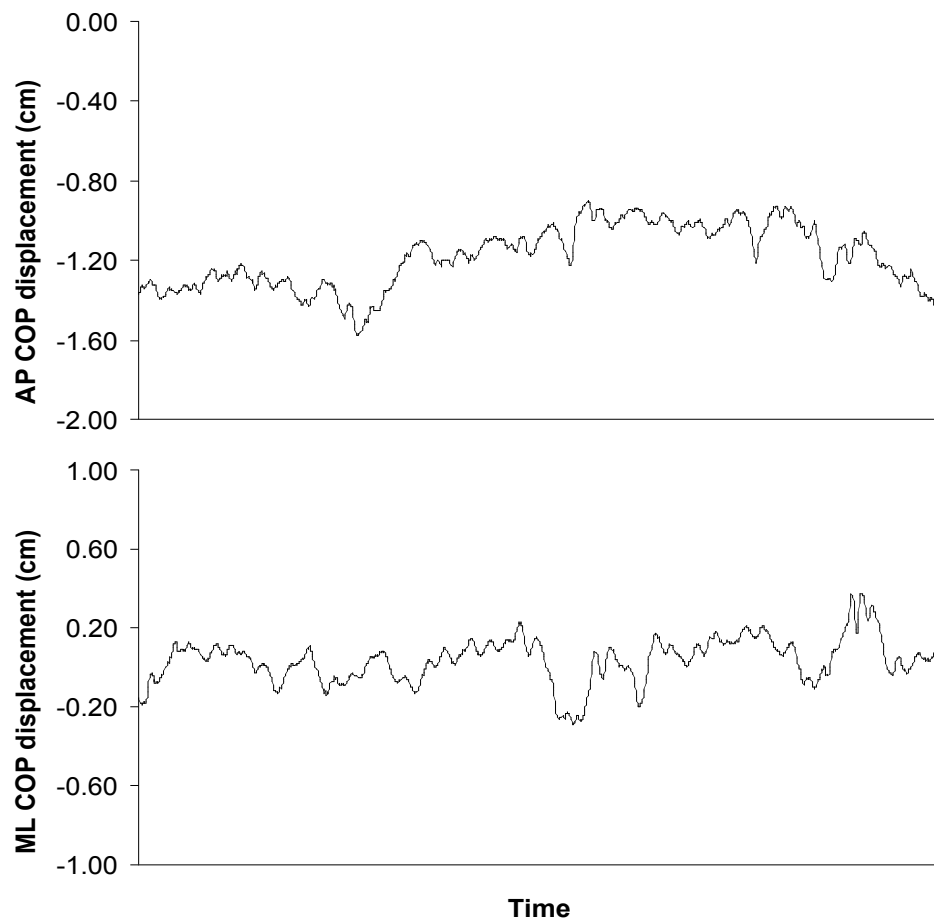


Figure 3.4. AP COP (top) and ML COP (bottom) times series for the COP profile shown in Figure 3.1.

RECURRENCE QUANTIFICATION ANALYSIS

RQA, a relatively new tool for the analysis of nonlinear dynamical systems, can be used to identify subtle patterns of recurrence in a data series (Webber & Zbilut, 1994, 1996; Zbilut & Webber, 1992; for a detailed tutorial, see Webber & Zbilut, Chapter 2). Time-delayed copies of a single scalar time series are used as surrogate variables to reconstruct a higher dimensional phase space. Through examination of the reconstructed phase space, RQA is able to detect system dynamics that are intrinsic to, though not readily apparent in, the one-dimensional time series. In the reconstructed phase space, the distances between all possible vectors are determined and used to create a distance matrix. Next, a recurrence matrix of recurrent points is generated from the distance matrix. Recurrent points are those points in the distance matrix that fall within a specified distance of one another.

A recurrence plot is simply a graphical depiction of the recurrence matrix. The recurrence plot is an autocorrelation plot of $x(t)$ with $x(i)$ along the abscissa and $x(j)$ along the ordinate. Only those points that satisfy $x(i) = x(j)$, defined as values of i and j that fall within a specified radius or distance of one another, are plotted. Visual inspection of recurrence plots may reveal patterns in the data not evident from examination of the time series. RQA uses pattern recognition algorithms (see discussion of quantification of qualitative features below) to quantify the recurrence features depicted in recurrence plots, and, therefore, is more objective than visual inspection of recurrence plots.

In the present chapter, we apply RQA to the COP data generated by the experiment described above to examine the effects of cognitive activity on postural fluctuations. An important characteristic of RQA is that, unlike other analytic techniques, it does not assume data stationarity. This is of particular relevance in the analysis of COP time series, which have been shown to be nonstationary—drift in the first (mean) and second (standard deviation) moments over time (Newell, 1998; Newell, Slobounov, Slobounova, & Molenaar, 1997; Schumann, Redfern, Furman, El-Jaroudi, & Chaparro, 1995). In addition, RQA requires no assumptions about data set size or distribution of the data.

RQA of the COP data from the present experiment was performed using recurrence software available free of charge from <http://homepages.luc.edu/~cwebber/>. *Recurrence Quantification Analysis* version 6.2 was used to conduct the present analyses, but a more recent version of the software is now available. The software includes 20 programs for examining recurrence in a single time series and cross-recurrence in two time series. All programs run in *MSDOS*, requiring the user to have a basic knowledge of how to work in a DOS environment. The *README.TXT* file is a valuable resource and should be read by all first-time users of the software. Toward the beginning of that file, programs are listed by purpose for which they are used. This provides a useful guide for selecting an appropriate program. For example, when the aim is to generate a recurrence plot, the user can look under the heading “2 programs display recurrence plots” and select from *RQD.EXE*, which is used to generate recurrence quantification plots for a single time series, and *KRQD.EXE*, which is used to generate cross-recurrence plots from two different files. Later

in the *README.TXT* file descriptions of each program detail program usage, input parameters that must be defined, and output that will be generated. The section of the *README.TXT* file titled “Mathematical Construction of the Recurrence Matrix” (see also Webber & Zbilut, Chapter 2) is a particularly helpful tool for understanding the process of RQA. In addition, near the end of the file, the creators of the software discuss several important points to consider in conducting RQA.

We used program *RQD.EXE* (Recurrence Quantification Display) to create recurrence plots. Figure 3.5 depicts recurrence plots for the AP COP and ML COP time series shown in Figure 3.4. The data used to generate these recurrence plots are available for download for the reader who wishes to reproduce these plots. As noted above, points plotted in the recurrence plot are those points determined to be “neighbors” in the reconstructed phase space, that is, COP values that are within a specified distance of one another. The basic features of recurrence plots and our choices of parameter values used to generate the plots with program *RQD.EXE* are explained below in the subsections entitled *Quantification of Qualitative Features of Recurrence Plots* and *Parameter Selection*. Additional information about the qualitative features of recurrence plots can be found in Riley, Balasubramaniam, and Turvey (1999).

Our plan was to use program *RQE.EXE* (Recurrence Quantification Epochs) to examine effects of cognitive task condition on five recurrence variables: %recurrence (%REC), %determinism (%DET), maxline (MAXL), entropy (ENT), and trend (TND).

In contrast to the program *RQD.EXE*, which we used to generate the recurrence plots, the output of *RQE.EXE* is entirely quantitative.

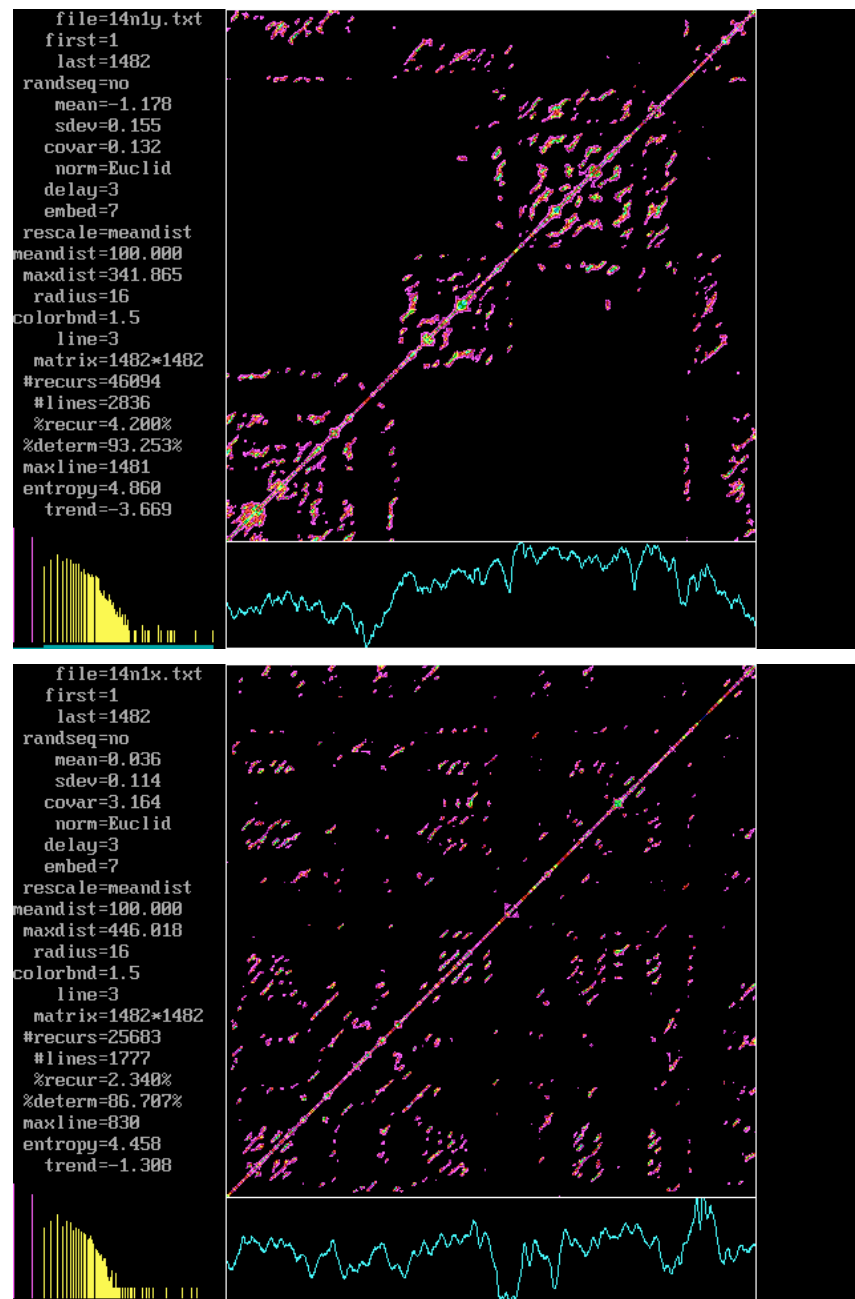


Figure 3.5. Recurrence plots for the AP COP (top) and ML COP (bottom) time series shown in Figure 3.4. The time series are plotted at the bottom of the figure. Recurrence parameters and recurrence output are listed to the left of the plot. Distribution of line lengths is graphed at the bottom left.

Recurrence variables are calculated from the upper triangular area of the recurrence plot, excluding the central diagonal, because the plot is symmetrical about the main diagonal. %REC is the percentage of data points that are recurrent, defined as those points falling within a distance specified by a selected radius value (see below). %DET, an index of degree of determinism, is the percentage of recurrent points that form diagonal lines in a recurrence plot (parallel to the central diagonal). In other words, %DET refers to the percentage of consecutive recurring points. The number of consecutive points needed to constitute a line is determined by the value selected for the line length parameter. MAXL is the length of the longest diagonal line, excluding the main diagonal. MAXL is inversely proportional to the largest positive Lyapunov exponent, and thereby provides a measure of the dynamical stability of the system. According to Webber and Zbilut (Chapter 2), “the shorter the [MAXL], the more chaotic (less stable) the signal.” ENT is calculated as the Shannon information entropy of a histogram of diagonal line lengths, and is an index of the complexity of the deterministic structure of the time series. TND provides a measure of the degree of system stationarity, with values of TND at or near zero reflecting stationarity and values deviating from zero indicating drift in the system.

Quantification of Qualitative Features of Recurrence Plots

Visual inspection of recurrence plots may be useful for a qualitative understanding of the quantitative recurrence measures described above. To this end, we have generated several recurrence plots for time series with known structure. In particular, we show recurrence plots for a simple sinusoid (Figure 3.6), the same sinusoid

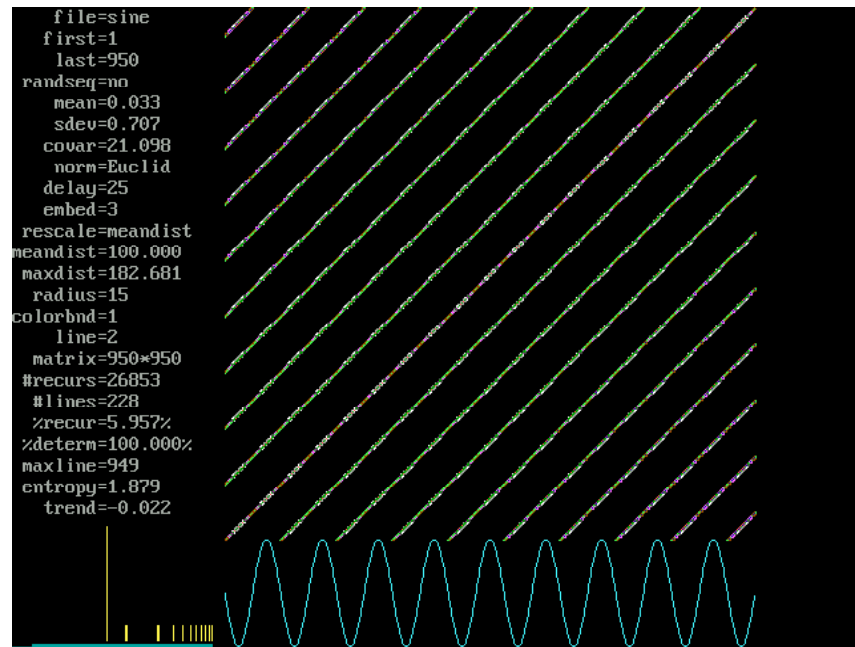


Figure 3.6. Recurrence plot for a simple sinusoid.

with superimposed white noise (Figure 3.7), the same sinusoid with a linear drift (Figure 3.8), a sample time series from a known complex mathematical system—the Lorenz attractor (Figure 3.9), and time series from two regimes of another mathematical system, the Hénon attractor (Figure 3.10). Comparison of the recurrence plots will help to illustrate what the quantitative recurrence measures actually mean.

%REC & %DET. Consider the simple sinusoid, which is an entirely deterministic signal, depicted in the bottom of Figure 3.6. By entirely deterministic, we mean that each value in the time series recurs and is part of a string of consecutive recurring values. This aspect of the time series is illustrated by every illuminated pixel in the recurrence plot corresponding to part of a diagonal line. This means

RQA of Postural Fluctuations

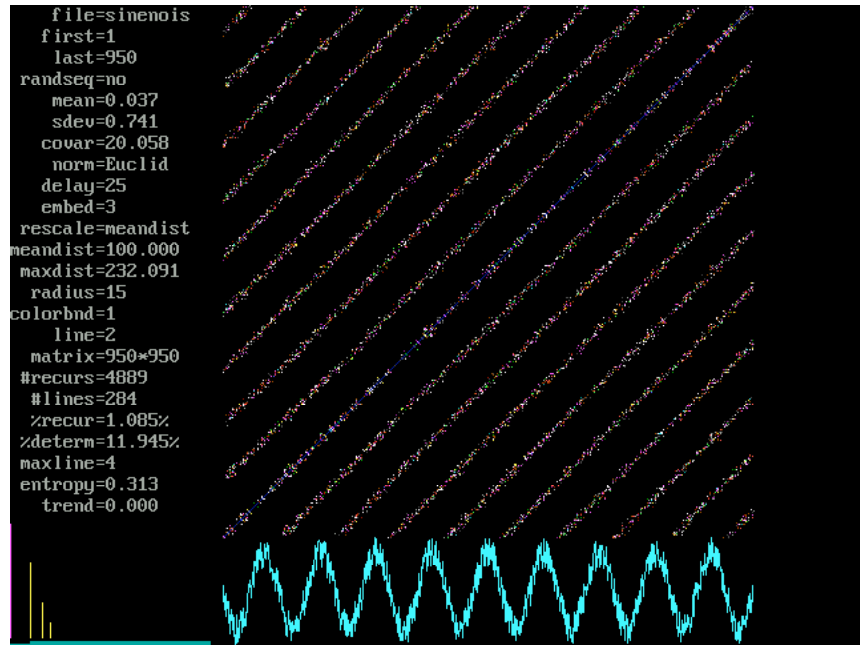


Figure 3.7. Recurrence plot for a sinusoid with superimposed white noise.

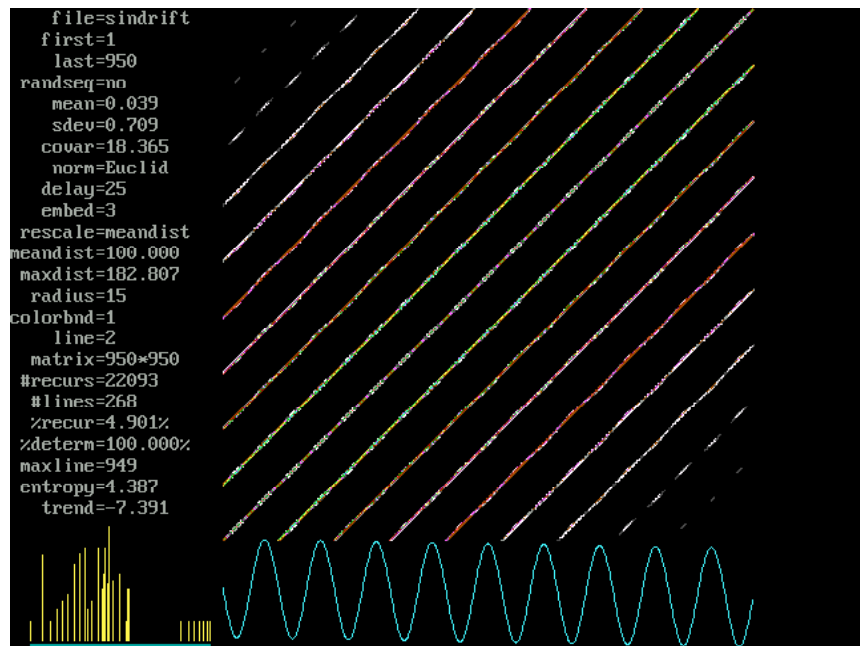


Figure 3.8. Recurrence plot for a sinusoid with linear drift.

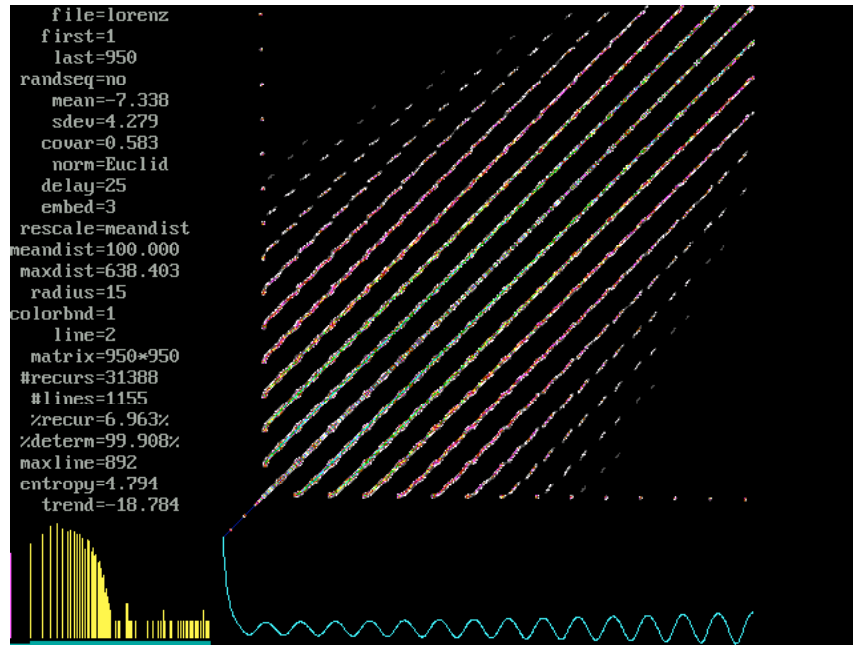


Figure 3.9. Recurrence plot for a time series from the Lorenz attractor.

that the proportion of recurring points that are part of a diagonal line is 100% (i.e., %DET = 100%). Note that just because every value in the time series recurs does not mean that every possible point in the recurrence plot is recurrent. In this particular example, of all of the possible locations that could be recurrent in a time series of a length of 950 data points ($950 \times 950 / 2 = 451,250$), 26,853 were recurrent (~6%) (the total number of possible recurrent points [950×950] is divided by 2 because only one of the triangular regions is used to calculate recurrence, since the plot is symmetrical about the main diagonal).

For the time series depicted in Figure 3.7, we no longer have an entirely deterministic signal, given that we have added a random component (white noise). Each value in the time series no longer recurs and each value that does recur is no longer necessarily part of a

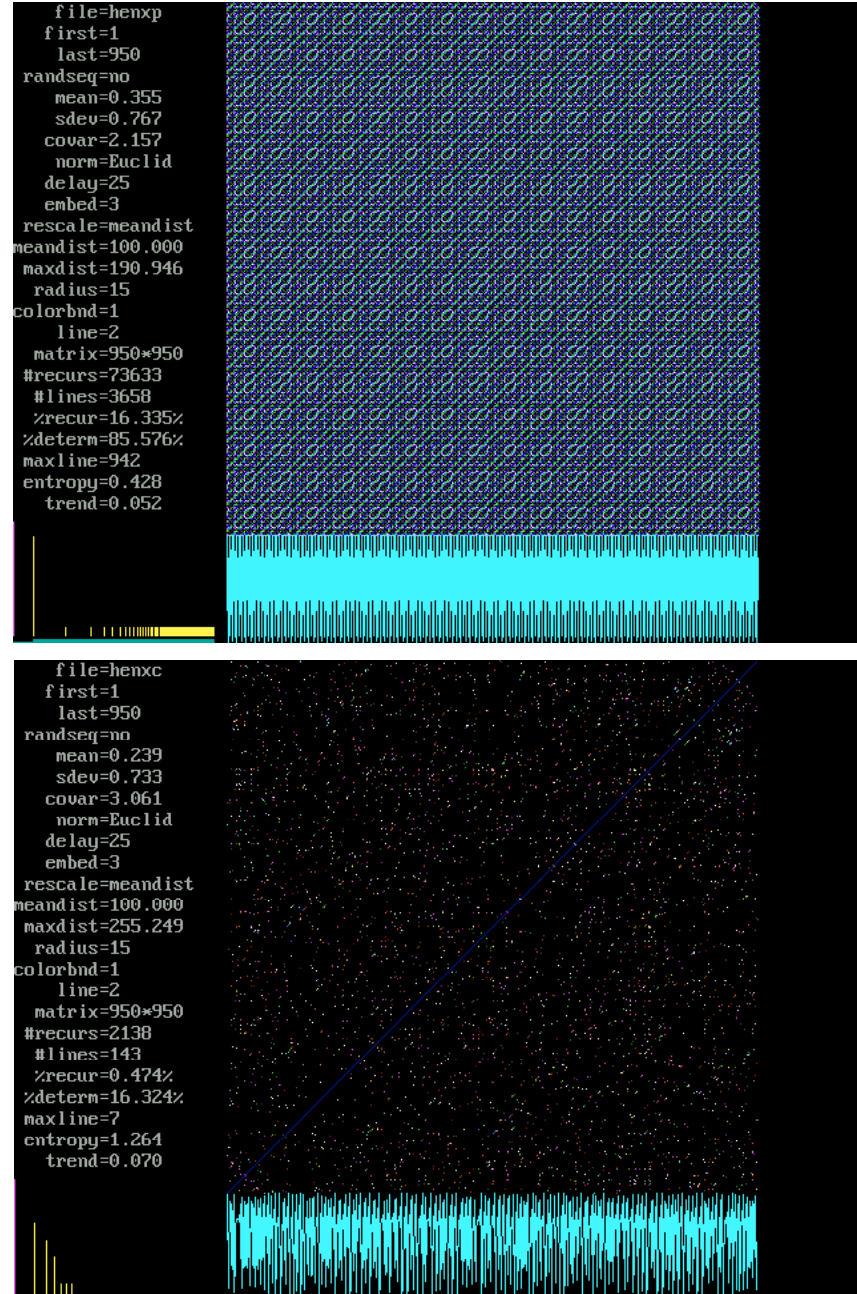


Figure 3.10. Recurrence plot for a times series from a periodic regime (top) and a chaotic regime (bottom) of the Hénon attractor.

diagonal line. The fact that each value in the time series no longer recurs is illustrated by fewer illuminated pixels in the plot (4,889 as compared to 26,853 in Figure 3.6) and a lower proportion of values recurring ($\sim 1\%$). The fact that the noisy signal in Figure 3.7 is no longer entirely deterministic is illustrated by the fact that fewer of the illuminated pixels form diagonal lines, which results in a lower value of %DET ($\sim 12\%$) than the signal in Figure 3.6.

TND. The time series depicted in Figure 3.8 is nonstationary—the mean state drifts (becomes lower in this case) over time. This was achieved simply by adding a monotonic decrease (a negatively sloped straight line) to the time series depicted in Figure 3.6. Note that we only have a modest change in %REC ($\sim 5\%$), and no change in %DET (100%) as compared to the time series in Figure 3.6 ($\sim 6\%$ and 100%, respectively). However, one can see a qualitative difference between the recurrence plots depicted in Figures 3.6 and 3.8.

Recall that the central diagonal corresponds to sameness in time. This location in the recurrence plot is ubiquitously recurrent because it represents comparison of a value to itself. But note that as one moves perpendicularly away from the central diagonal, this represents deviation in time. For example, as one moves upward and left away from the diagonal, this means that one is comparing a point early in the time series (indicated by a value on the x-axis near the origin) to a point later in the time series (indicated by a value on the y-axis near the extreme). As one moves perpendicularly away from the central diagonal in Figure 3.8, the pixel density decreases. This occurs because over time there is a drift in the mean state of the time series. The average value of the first 100 points in the time series is

approximately 0.09, while the average of the last 100 points is approximately -0.09. The color density does not change, however, in the recurrence plot depicted in Figure 3.6. This qualitative aspect of the recurrence plot is quantified by the measure of trend (TND)—the slope of %REC as a function of distance away from the diagonal. Note that TND for Figure 3.8 is considerably different than zero (~7) while the value of TRD for Figure 3.6 is approximately equal to zero.

ENT. The time series depicted in Figure 3.9 is a sample of data generated from the Lorenz model. The Lorenz system is a nonlinear, chaotic system that would be considered a complex system by most. The equations representing the Lorenz system and the true and reconstructed phase spaces of the system may be seen in Shockley (Chapter 4). We have selected sample data from this system to illustrate how recurrence analysis may be used to quantify the complexity of a time series. Note that in the time series depicted in the bottom of Figure 3.9 the system appears to be somewhat periodic, as indicated by the peaks and valleys occurring at similar periods. However, the amplitude of the signal changes over time and abrupt shifts in the value of the system occur at irregular intervals (compare the first part of the time series to the later parts). Note that most of the illuminated pixels form diagonal lines (as indicated by %DET = 99%) and that we see a similar proportion of recurrent points as in Figure 3.6 (~7%). However, the recurrence plot in Figure 3.9 looks different than the recurrence plot in Figure 3.6. This distinction between the plots can be captured most readily by the frequency distribution of line lengths shown in the lower left of each figure. The distribution of line lengths for the Lorenz system (Figure 3.9) has a richer variety than that for the

simple sinusoid (Figure 3.6). This variety of structure is what is meant by complexity in recurrence analysis. This aspect of the time series is quantified by the Shannon entropy (ENT ; the negative sum of the normalized \log_2 probabilities [P] of lines corresponding to given line lengths) of the line length distributions in question (see Equation 2.11 in Webber & Zbilut, Chapter 2). Note that the entropy for the Lorenz system ($ENT = \sim 5$) is greater than the entropy for a simple sinusoid ($ENT = \sim 2$), indicating that the Lorenz system is more complex than a simple sinusoid.

MAXL. To illustrate the meaning of the recurrence measure maxline (MAXL), we have selected data sets generated from the Hénon system. The Hénon system is a model of the dynamics of stars moving within galaxies. It is governed by the following two equations of motion:

$$\dot{x} = y + 1 - ax^2 \quad [3.1]$$

$$\dot{y} = bx \quad [3.2]$$

where x and y correspond to the dimensions of change, x and y with overdots correspond to rate of change along those dimensions, and a and b are parameters.

One of the interesting features of the Hénon system is that depending on the values of the parameters (a and b) the Hénon system may exhibit behavior that is highly predictable (periodic) or chaotic behavior that is only predictable in the very short term. Figure 3.10 shows recurrence plots of a periodic regime (oscillation among 16 values; e.g., $a = 1.055$, $b = 0.3$) and a chaotic regime of the Hénon

system (e.g., $a = 1.4$, $b = 0.3$) (the data sets used in the present example are provided with the RQA software at <http://homepages.luc.edu/~cwebber/>). By definition, the chaotic regime is less stable than the periodic regime. By stability we mean that two trajectories that are initially nearby one another stay nearby one another longer in a more stable system than in a less stable system. MAXL has been shown to be sensitive to the stability of the system in question (Eckmann, Kamphorst, & Ruelle, 1987).¹ The larger MAXL, the more stable the system—nearby trajectories diverge less quickly than for a system with a smaller MAXL. For the chaotic regime of the Hénon attractor the longest diagonal line is quite short ($\text{MAXL} = 7$) as compared to the longest diagonal line for the periodic regime ($\text{MAXL} = 942$). While it is the case that MAXL will change considerably depending on the system under scrutiny (as can be seen by comparison of MAXL values for Figures 3.6-3.10), what is of interest is how MAXL changes within the same system (in this case the Hénon system) under different conditions.

Parameter Selection

Prerequisite to generating plots and calculating recurrence variables is the selection of appropriate settings for seven parameters:

¹ Lyapunov exponents quantify the exponential rate of divergence of nearby trajectories along a given dimension in the system. A negative Lyapunov exponent quantifies the average rate of convergence of trajectories over time, while positive Lyapunov exponents characterize the average rate of divergence over time. For a highly stable system (e.g., periodic systems), two trajectories that are initially nearby one another will continue to be nearby one another at any given later point in time. This means that the Lyapunov exponent would be at or near zero (i.e., no divergence over time). One hallmark of chaotic systems, however, is that they have at least one positive Lyapunov exponent (meaning that along at least one dimension, two trajectories that are initially nearby one another will diverge exponentially over time). Chaotic systems that exhibit bounded regions in which trajectories unfold (e.g., the Lorenz attractor or the Henon attractor for certain parameter ranges) also have at least one negative Lyapunov exponent. MAXL has been shown to be inversely proportional to the largest positive Lyapunov exponent (larger MAXL smaller value of Lyapunov exponent; see Eckmann, Kamphorst, & Ruelle, 1987).

Embedding dimension, delay, range, norm, rescaling, radius, and line length (see Webber & Zbilut, Chapter 2). Selection of these parameter values is challenging. Although some guidelines are available, there are as of yet no absolute standards for identifying the most appropriate parameter values. A summary of the decision making that was involved in our choice of parameters follows.

Selection of some parameters is more difficult than others. Choosing a proper embedding dimension, delay, and radius are among the most challenging decisions that must be made. We followed the approach described by Zbilut and Webber (1992) and used by Riley et al. (1999) to select values for those three parameters. The general strategy is to calculate RQA measures for a range of parameter values, and select a value from a range in which small changes in parameter settings result in small, continuous changes in the RQA measures. To follow that strategy, we enlisted program *RQS.EXE* (Recurrence Quantification Scale), which "...scales recurrence quantifications for a single epoch of data by incrementing parameter values over specified ranges" (Webber, 2004, p. 6). In the following paragraphs, we describe first the decision making involved in selecting a range of parameters for embedding dimension, delay, and radius for use in *RQS.EXE*, and next the choice of a single setting for each parameter.

Embedding Dimension. Embedding dimension specifies the n-dimensions of the reconstructed phase space, that is, the dimension into which the dynamic of the system under study will be projected (see discussion of delay below). Selecting an embedding dimension that is too high can amplify the effects of noise. Choosing an

embedding dimension that is too low will result in underdetermination, that is, the dynamics of the system will not be fully revealed. Webber (2004) suggested, for physiological data, starting with embedding dimensions between 10 and 20 and working downward. Investigators applying RQA to the study of COP data have reported embedding dimension 8 (Schmit et al., submitted), 9 (Riley & Clark, 2003) and 10 (Balasubramaniam, Riley, & Turvey, 2000; Riley et al., 1999). Based on Webber's suggestion and previous papers, we decided to examine RQA output for embedding dimensions 7 through 10.

Delay. As mentioned previously, time-delayed copies of the data series are used as surrogate variables to project the data into higher-dimensional space. The delay parameter specifies the time lag to use in reconstructing that phase space. For example, imagine a time series for which we selected a delay (τ) of 10 and embedding dimension of 3. Our first embedding dimension [$x(t)$] in the reconstructed phase space would start at data point 1 of the original time series (x), the second embedding dimension [$x(t + \tau)$] would start at data point 11, and the third embedding dimension [$x(t + 2\tau)$] would start at data point 21. A two-dimensional phase space could be constructed the same way that one plots a two-dimensional scatterplot to evaluate the relationship between two variables in correlation or regression, the two variables in this case being $x(t)$ and $x(t + \tau)$. One could add a third (or higher) dimension to the phase space in the same fashion (see Figure 4.4 in Shockley, Chapter 4). Previous studies in which COP data were sampled at 100 Hz used time delays ranging between 0.04 s and 0.09 s. Considering the sampling rate of the force plate used in the present study (50 Hz), delays of 2 to 5 data points corresponded to time delays

of 0.04 to 0.10 seconds. We decided to examine RQA output for delays ranging between 2 and 10 data points.

Radius. The radius parameter defines the Euclidean distance within which points are considered neighbors in the reconstructed phase space. Said differently, the radius sets the threshold for recurrence. The larger the radius, the more points will be considered recurrent. As a general guideline, a radius should be selected such that %REC remains low (see Webber & Zbilut, Chapter 2). We wanted a radius that was small enough to yield relatively low %REC (no larger than 5%), but not so small as to produce a floor effect with values of %REC near or at 0.0%. Other investigators have used a radius of 10 or 11 in the analysis of COP data (Balasubramaniam et al., 2000; Riley et al., 1999; Riley & Clark, 2003). We decided to examine RQA output for radius settings ranging between 10 and 26.

Norm. The norm parameter determines the method used for computing distances between vectors in the reconstructed phase space. We selected Euclidean normalization, which is consistent with previous studies using RQA to examine COP data (see Riley et al., 1999; Riley & Clark, 2003).

Rescale. The rescale parameter determines the method used to rescale the distance matrix. Although rescaling to maximum distance is a typical choice, we decided to rescale relative to mean distance. Mean distance rescaling minimizes the influence of an outlier, which can be a problem when rescaling to maximum distance. An assumption of rescaling to mean distance, however, is that the distribution of the distances is Gaussian.

Range. The range of data points included in the recurrence analysis is specified by setting the first point, P_{start} (the data point in the time series at which the analysis will start), and the last point, P_{end} (the data point in the time series at which the analysis will end). We wanted to include as many of the data points in the time series as possible in our recurrence analysis. For that reason, we input the first point as 1 and the last point as 1410, thereby selecting the largest range possible, given constraints due to the number of data points in the time series ($N = 1500$), maximum embedding dimension ($M = 10$), and maximum delay ($\tau = 10$). The last data point was determined by $P_{\text{end}} = N - (M - 1) \times \tau$. This guarantees the use of the maximal number of data points and the same number of data points within each surrogate dimension in the phase space. When using *RQS.EXE*, however, we did not actually have to compute P_{end} , because when the program prompts the user to input LAST (P_{end}), it specifies the last possible point in the time series that could be used. We simply input that last possible point, 1410, as our value for P_{end} .

Line Length. Line length specifies the number of consecutive recurrent points required to define a line segment. Often, line length is set at two points. Specifying a line length of more than two points yields increasingly conservative estimates of the deterministic structure in the system. In the present study, line length was set to three points.

Having determined a range of parameter settings for embedding dimension, delay, and radius, and selected settings for norming method, rescaling method, range, and line length, our next step was to choose (at random) a few trials from each experimental condition and use program *RQS.EXE* to compute recurrence measures for the selected

parameter ranges. To reiterate, our purpose in running *RQS.EXE* on a sample of experimental trials was to generate recurrence measures for a range of embedding dimensions, delays, and radius values. As noted above, we set minimum embedding dimension at 7, maximum embedding dimension at 10; minimum delay at 2 samples, maximum delay at 10 samples; and minimum radius at 10, maximum radius at 26. Table 3.1 lists each of the parameter settings we selected in running *RQS.EXE*.

We inspected the recurrence measures that were generated by *RQS.EXE* for our sample of trials to decide on specific settings for embedding dimension, delay, and radius to be used in carrying out the RQA of all experimental trials. To recap, we were looking for small changes in parameter settings yielding smooth changes in output measures, %REC values ranging between 1% and 5%, and absence of ceiling or floor effects on %DET. We created in *Matlab* (Mathworks, Inc., Natick, MA) a series of surface plots to visualize changes in %REC as a function of embedding dimension, delay, and radius. A separate plot was created for each of the four embedding dimensions under examination (see Figure 3.11), with radius on the x-axis, delay on the y-axis, and the dependent variable %REC on the z-axis. The surface plots in Figure 3.11 illustrate well that in spite of the fact that increasing values of radius yielded higher %REC, each of the plots looks qualitatively similar. That is, there are no qualitative differences in the patterns of %REC (i.e., the shape of each surface) for this range of parameter settings. The fact that incremental changes in parameter values yield smooth (not abrupt) changes in %REC (e.g., steady increases in %REC with increases in radius or steady decreases in

Table 3.1. Parameter settings selected when prompted by program RQS.EXE. MIN = minimum; MAX = maximum; RANDSEQ = randomize data sequence. See README.TXT file accompanying software for further explanation of parameters listed above (Webber, 2004). NORM value of 3 corresponds to Euclidean normalization. Selection of RANDSEQ n is a “no” response to the option of randomly sequencing points in the data set, thereby retaining the original order of points in the time series. Rescale value of 2 instructs the program to rescale the matrix to mean distance.

Parameter	Setting
DELAY MIN	2
DELAY MAX	10
EMBED MIN	7
EMBED MAX	10
NORM	3
FIRST	1
LAST	1410
RANDSEQ	n
RESCALE	2
RADIUS MIN	10
RADIUS MAX	26
RADIUS STEP	1
LINE	3

%REC with increases of embedding dimension) suggests that using a set of parameters within the selected range will not yield notable changes in %REC that are artifacts of parameter selection. For additional information about surface plots, see Shockley’s (Chapter 4)

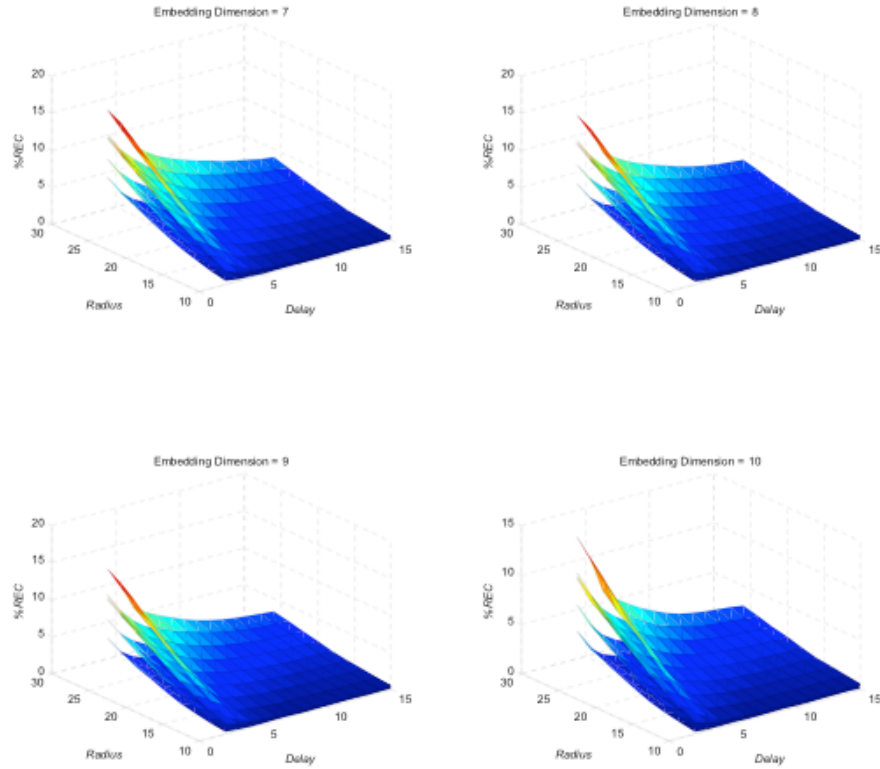


Figure 3.11. Surface plots for embedding dimensions 7-10, showing steady increase in percentage of recurrent points (%REC) with increasing values of radius, but no apparent difference in the pattern of %REC across the four plots.

application of cross-recurrence analysis. Based on our inspection of the surface plots and the numerical recurrence output generated by program *RQS.EXE*, we selected the following parameter settings: Embedding dimension of 7, time delay of 3 samples (corresponding to a 0.06 s lag), and radius of 16. Our decision to set the radius parameter at 16 means that points falling within 16% of the mean Euclidean distance of each other would be considered recurrent. As can be seen in the surface plots, this radius ensures that our %REC values will be in

our target range of 1-5%. It is important to note that had we selected slightly different parameters, we would still have seen the same basic pattern in the results, although the particular magnitudes of recurrence measures would have scaled up or down.

Our next step was to run the RQA with the selected parameter settings on the entire set of experimental trials. Program *RQE.EXE* was used to compute the five recurrence variables of interest, %REC, %DET, MAXL, ENT, and TND. As a practical note, recurrence analysis can take a long time (hours) to run, depending on file size, number of trials, and processor speed. An advantage of using *RQE.EXE* as opposed to *RQD.EXE*, for example, is that the former allows multiple analyses to be executed in batch mode, rather than waiting for each file to be analyzed and typing the next command for the next file to be analyzed. Computations were performed using the following parameter settings: Delay = 3, embedding dimension = 7, range = 1–1482, norm = Euclidean, rescaling = mean distance, radius = 16, and line length = 3. The program *RQEP.EXE* was used to generate a parameter file, to be called by the batch file commands, containing those parameter selections. An ASCII (text), tab-delimited batch file (*filename.bat*) was set up such that each row corresponded to the *MSDOS* command for analyzing one file using *RQE.EXE*. The number of rows corresponded to the number of files to be analyzed (see *README.TXT* file for complete instructions). Program run time for the present data was approximately four hours. Mean values for the recurrence measures were calculated for the two trials in each condition. Separate ANOVAs were conducted on each recurrence measure for AP COP and ML COP time series.

After the RQA was complete for all of the experimental trials, we reran the RQA for six randomly chosen trials using the same parameter settings, but selecting the option to randomize the order of the data points. Comparing the RQA findings of the randomly shuffled data and the normally sequenced data provides the means to confirm our choice of parameter settings as appropriate for revealing the deterministic structure present in the original time series (see Webber & Zbilut, Chapter 2).

Figure 3.12 depicts the recurrence plots generated with random shuffling of data from the time series in Figure 3.4. Although the values in the time series of Figure 3.12 (just below the recurrence plot) are exactly the same as those for the time series in Figure 3.5, because they are randomly shuffled, nearness in time no longer necessarily means nearness in value. For example, in a typical time series, the value for the 10th data point will be reasonably close to the value for the 11th data point, simply because a person cannot instantaneous move the body across large distances. However, when the values are randomly shuffled, the 100th data point from the original time series could end up next to the 10th data point of the original time series. When the data points from the new, randomly shuffled time series are connected by a line for plotting, the time series now looks extremely densely packed as compared to the original, in spite of the fact that none of the values have changed. This, however, is simply an artifact of “connecting the dots,” as it were.

What is more important than comparing the time series of Figures 3.5 and 3.12 is comparing the recurrence plots. Recall that only recurring points are plotted in a recurrence plot. Visual comparison of

RQA of Postural Fluctuations

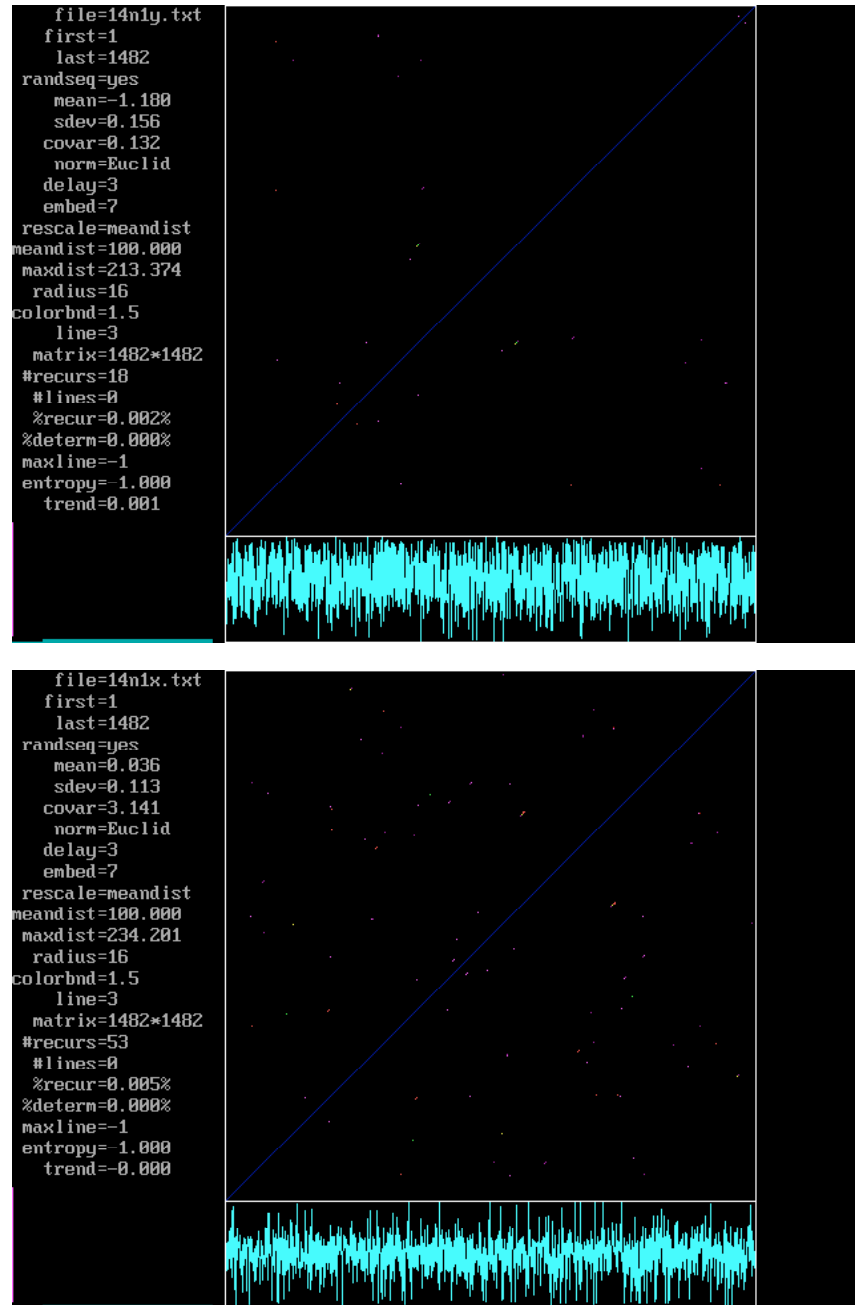


Figure 3.12. Recurrence plots for the AP COP (top) and ML COP (bottom) data sets shown in Figure 3.4, but randomly shuffled. The data series (following random shuffling) are shown at the bottom of the figure; recurrence parameters and recurrence output are listed to the left of the plot. Note that the same recurrence parameters were used to generate recurrence plots for the original times series (see Figure 3.5) and the randomly shuffled data sets.

the recurrence plots in Figures 3.5 and 3.12 shows that fewer points are recurrent for the randomly shuffled data and that almost none of those recurrent points form diagonal lines. This qualitative change is reflected quantitatively by the fact that, for the randomly shuffled data, $\%REC < 0.01\%$ and $\%DET < 0.001\%$. Randomizing the data reduced the number of recurrent points, but, perhaps more importantly, it eliminated the deterministic structure of the original time series. The interested reader can reproduce the plots shown in Figure 3.12 by using the data that accompany this chapter and running program *RQD.EXE* with the parameter settings listed previously (and depicted at the left side of the plots in Figure 3.12) and selecting ‘y’ for the *randomize data sequences* option.

Results of RQA

For AP COP, ANOVA revealed a main effect of cognitive task condition on $\%DET$, $F(3, 57) = 3.52$, $p < .05$, which is shown in Figure 3.13a. $\%DET$ was greater for counting back by 3s ($M = 88.70$) than quiet standing ($M = 85.65$) and digit reversal ($M = 83.61$). This finding suggests that the temporal structure of AP postural fluctuations became more regular as the attentional demands of the cognitive task increased. Recalling the results of the traditional analysis of AP COP data (Figures 3.3b and 3.3d) in view of the observed changes in $\%DET$ for the AP COP time series, we see that although the amplitude and variability of postural sway increased with greater attentional demands of the concurrent cognitive task, the postural fluctuations became more deterministic (regular). ANOVAs on $\%REC$, MAXL, ENT, and TND did not reveal any other effects of cognitive task condition for the AP COP time series.

RQA of Postural Fluctuations

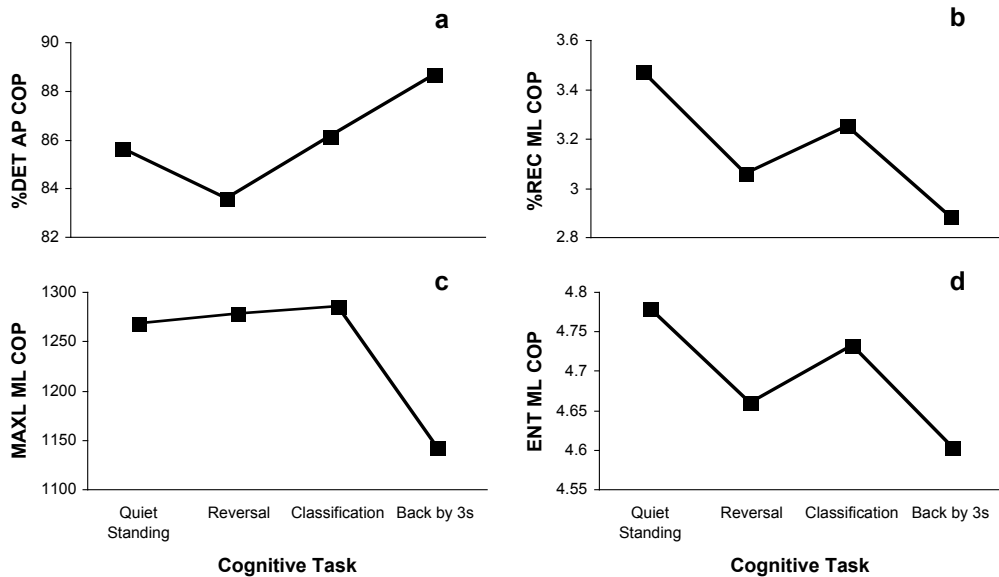


Figure 3.13. Results of RQA for all experimental trials. (a) Percent determinism (%DET) for AP COP as a function of cognitive task condition. For ML COP, (b) Percentage of recurrent points (%REC), (c) maxline (MAXL), and (d) entropy (ENT) as a function of cognitive task condition.

For ML COP, ANOVA on %REC showed that the effect of cognitive task condition approached significance, $F(3, 57) = 2.64, p < .06$ (see Figure 3.13b). Pair-wise comparisons revealed a lower percentage of recurrent points ($p < .05$) for the counting back by 3s cognitive task ($M = 2.89$) than for digit classification ($M = 3.25$) and quiet standing ($M = 3.47$). Generally, ML COP fluctuations were less recurrent when performing concurrent cognitive and postural tasks than when simply standing.

ANOVA on MAXL of the ML COP time series revealed a main effect of cognitive task condition, $F(3, 57) = 2.83, p < .05$. MAXL was shorter for counting back by 3s ($M = 1142.9$) than for digit classification ($M = 1286.8$) and digit reversal ($M = 1278.3$). This finding, depicted in

Figure 3.13c, suggests that the temporal structure of the ML COP was less mathematically stable when the cognitive task required higher attentional demands.

Figure 3.13d shows the significant main effect of cognitive task condition on ENT of the ML COP data, $F(3, 57) = 4.25, p < .01$. ENT was lower for counting back by 3s ($M = 4.60$) than for digit classification ($M = 4.73$) and quiet standing ($M = 4.78$). This finding suggests the deterministic structure of the ML COP was less complex for the cognitive task of highest attentional demand.

ANOVAs for the ML COP data did not indicate an effect of cognitive task condition on the recurrence measures of %DET and TND.

GENERAL DISCUSSION

The present research highlights the utility of RQA for the study of postural fluctuations. Using a traditional approach to the analysis of COP data, we found that total COP excursion, as well as the range and variability of AP and ML COP motion, were impacted by attentional demands in a similar manner. Results of the traditional analyses showed that performing a concurrent cognitive task increased the magnitude and variability of postural sway. These findings could lead one to conclude that carrying out an unrelated but concurrent cognitive task compromises postural stability.

The RQA results suggest an alternative interpretation. Attentional demands impacted postural sway, but not necessarily in the form of a decline in the effectiveness of the postural control system. Examination of the temporal structure of postural fluctuations revealed that attentional demands influenced AP COP and ML COP in different ways.

Whereas with higher attentional demands fluctuations in ML COP became less recurrent, less stable, and less complex, AP COP fluctuations became more deterministic. What might explain these observed differences in recurrence patterns in the two COP component directions? One possibility is that the RQA findings reflect a strategy being used by the central nervous system (CNS) to optimize postural control. Recall the stance position maintained by study participants, which is shown in Figure 3.2. In keeping with instructions to stand with feet together, participants adopted a narrow base of support during testing. Thus, it is likely that the perceived limit of stability (PLOS—the distance an individual can sway without losing balance or taking a protective step) was smaller for ML motion than for AP motion. Increases in ML COP motion may have presented a greater threat to postural stability than AP COP motion, since increased ML motion would bring the ML COP closer to the PLOS. The changes in recurrence patterns of ML COP data series may follow from the increased COP motion in that direction. Of note, spontaneous ML postural sway, rather than AP sway, has been shown to be predictive of fall risk in older adults (Lord, Rogers, Howland, & Fitzpatrick, 1999; Maki, Holliday, & Topper, 1994).

Why wouldn't the CNS simply reduce sway range and variability as a way of promoting postural stability under conditions of greater attentional demand? The observed increase in the deterministic structure of AP COP may be a more efficient and more effective means of optimizing postural control. Sway range and variability are important aspects of exploratory postural behavior—sway is “exploratory” because it generates stimulation regarding the current state of postural

stability. The regularization of AP motion could be a strategy that simplifies the problem of postural control without sacrificing the pick-up of perceptual information made available through spontaneous postural sway. In short, rendering AP COP motion more deterministic may be one approach by which the postural system adjusts to the attentional demands of a concurrent cognitive task.

To summarize, it is difficult to interpret the results of the traditional analysis of COP data in terms other than a classical dual-task effect, in which concurrent performance of a cognitive task brings about a decrement in the ability of the CNS to control posture. Results of RQA, however, suggest adaptation of the postural system (perhaps proactively as well as reactively) to changing task demands. Although a full understanding of the findings reported here must await further research, a few points are clear. The results of the RQA brought to light dynamical processes inherent in postural control that are not evident in summary measures of COP path magnitude and variability. In addition, our findings offer further evidence that AP and ML COP motion can be affected differentially in response to varying task requirements (Balasubramaniam et al., 2000). Most importantly, the present study supports the notion that the response of the postural control system to dual-task requirements is one of adaptation not deterioration.

CONCLUSION

A conventional approach to the analysis of COP data revealed increases in measures of COP path magnitude and variability during performance of a concurrent cognitive task. Those findings are consistent with the notion that dual-tasking compromises postural

control. Also of note, AP COP and ML COP summary measures were impacted in a similar manner. In a second stage of data analysis, RQA revealed changes in the dynamical properties of postural sway brought about by concurrent performance of cognitive and postural tasks. Among the observed changes were differential effects on the AP and ML components of postural fluctuations. The results of RQA suggest that the postural control system adapts, rather than deteriorates, in response to changing attentional requirements. The analytic tools available through RQA promise insight into the mechanisms and processes underlying postural control not accessible with a conventional approach to the study of postural sway.

AUTHOR NOTE

This work was supported in part by a Patrick and Catherine Weldon Donaghue Medical Research Foundation grant awarded to G. L. Pellechia. The authors thank Michael Riley for many helpful discussions about RQA parameter settings for COP data.

REFERENCES

- Balasubramaniam, R., Riley, M. A., & Turvey, M. T. (2000). Specificity of postural sway to the demands of a precision task. *Gait and Posture*, 11, 12-24.
- Dault, M. C., Geurts, A. C. H., Mulder, T. W., Duysens, J. (2001). Postural control and cognitive task performance in healthy participants while balancing on different support-surface configurations. *Gait and Posture*, 14, 248-255.
- Derave, W., De Clercq, D., Bouckaert, J., & Pannier, J. L. (1998). The influence of exercise and dehydration on postural stability. *Ergonomics*, 41, 782-789.
- Eckmann, J. P., Kamphorst, S. O., Ruelle, D. (1987). Recurrence plots of dynamical systems. *Europhysics Letters*, 5, 973-977.
- Gravelle, D. C., Laughton, C. A., Dhruv, N. T., Katdare, K. D., Niemi, J. B., Lipsitz, L. A., & Collins, J. J. (2002). Noise-enhanced balance control in older adults. *Neuroreport*, 13, 1853-1856.

Guerraz, M., Thilo, K., V., Bronstein, A. M., & Gresty, M. A. (2001). Influence of action and expectation on visual control of posture. *Cognitive Brain Research*, 11, 259-266.

Kerr, B., Condon, S. M., & McDonald, L. A. (1985). Cognitive spatial processing and the regulation of posture. *Journal of Experimental Psychology: Human Perception and Performance*, 11, 617-622.

Lajoie, Y., Teasdale, N., Bard, C., & Fleury, M. (1993). Attentional demands for static and dynamic equilibrium. *Experimental Brain Research*, 97, 139-144.

Lord, S. R., Rogers, M. W., Howland, A., & Fitzpatrick, R. (1999). Lateral stability, sensorimotor function and falls in older people. *Journal of the American Geriatrics Society*, 47, 1077-1081.

Maki, B. E., Holliday, P. J., & Topper, A. K. (1994). A prospective study of postural balance and risk of falling in an ambulatory and independent elderly population. *Journals of Gerontology: Medical Science*, 49, M72-M84.

Maylor, E. A., Allison, S., & Wing, A. M. (2001). Effects of spatial and nonspatial cognitive activity on postural stability. *British Journal of Psychology*, 92, 319-338.

Pellechia & Shockley

Maylor, E. A., & Wing, A. M. (1996). Age differences in postural stability are increased by additional cognitive demands. *Journals of Gerontology: Series B, Psychological Sciences and Social Sciences*, 51B, P143-P154.

Newell, K. M. (1998). Degrees of freedom and the development of postural center of pressure profiles. In K. M. Newell & P. C. M. Molenaar (Eds.), *Applications of Nonlinear Dynamics to Developmental Process Modeling* (pp. 63-84). Mahwah, NJ: Erlbaum.

Newell, K. M., Slobounov, S. M., Slobounova, B. S., & Molenaar, P. C. M. (1997). Short-term non-stationarity and the development of postural control. *Gait and Posture*, 6, 56-62.

Pellecchia, G. L., & Turvey, M. T. (2001). Cognitive activity shifts the attractors of bimanual rhythmic coordination. *Journal of Motor Behavior*, 33, 9-15.

Pellecchia, G. L. (2003). Postural sway increases with attentional demands of concurrent cognitive task. *Gait and Posture*, 18, 29-34.

Polonyova, A., & Hlavacka, F. (2001). Human postural responses to different frequency vibrations of lower leg muscles. *Physiological Research*, 50, 405-410.

Posner, M. I. (1964). Information reduction in the analysis of sequential tasks. *Psychological Review*, 71, 491-504.

Posner, M. I., & Rossman, E. (1965). Effect of size and location of information transforms upon short-term retention. *Journal of Experimental Psychology, 70*, 496-505.

Riley, M. A., Balasubramaniam, R., & Turvey, M. T. (1999). Recurrence quantification analysis of postural fluctuations. *Gait and Posture, 9*, 65-78.

Riley, M. A., & Clark, S. (2003). Recurrence analysis of human postural sway during the sensory organization test. *Neuroscience Letters, 342*, 45-48.

Schmit, J. M. , Riley, M. A., Dalvi, A. , Sahay, A., Shear, P. K., Shockley, K. D., & Pun, R. Y.-K. (submitted). Recurrence quantification analysis of postural sway in Parkinson's disease.

Schumann, T., Redfern, M. S., Furman, J. M., El-Jaroudi, A., & Chaparro, L. F. (1995). Time-frequency analysis of postural sway. *Journal of Biomechanics, 27*, 603-607.

Stelmach, G. E., Zelaznik, H. N., & Lowe, D. (1990). The influence of aging and attentional demands on recovery from postural instability. *Aging, 2*, 155-161.

Vuillerme, N., Forestier, N., & Nougier, V. (2002). Attentional demands and postural sway: the effect of the calf muscles fatigue. *Medicine and Science in Sports and Exercise, 34*, 1907-1912.

Vuillerme, N., Nougier, V., & Teasdale, N. (2000). Effects of a reaction time task on postural control in humans. *Neuroscience Letters, 291*, 77-80.

Webber, C. L., Jr. (2004). Introduction to recurrence quantification analysis. *RQA version 8.1 README.TXT*. Retrieved February 13, 2004, from <http://homepages.luc.edu/~cwebber/>

Webber, C. L., Jr., & Zbilut, J. P. (1994). Dynamical assessment of physiological systems and states using recurrence plot strategies. *Journal of Applied Physiology, 76*, 965-973.

Webber, C. L., Jr., & Zbilut, J. P. (1996). Assessing deterministic structures in physiological systems using recurrence plot strategies. In M. C. K. Khoo (Ed.), *Bioengineering Approaches to Pulmonary Physiology and Medicine* (pp. 137-148). New York: Plenum Press.

Woollacott, M., & Shumway-Cook, A. (2002). Attention and the control of posture and gait: A review of an emerging area of research. *Gait and Posture, 16*, 1-14.

Zbilut, J. P., & Webber, C. L., Jr. (1992). Embeddings and delays as derived from quantification of recurrence plots. *Physics Letters A, 171*, 199-203.